Vol 11 No 3, March 2002
1009-1963/2002/11(03)/0272-05
Chinese Physics
© 2002 Chin. Phys. Soc.
and IOP Publishing Ltd

Phase transition and pitting corrosion behaviour for Mo-implanted aluminium*

Zhang Tong-He(张通和)[a)†], Wu Yu-Guang(吴瑜光)[a)],
Liu Pei-Ying(刘培英)[b)], and Qian Wei-Dong(钱卫东)[a)]

[a)] *Key Laboratory in University for Radiation Beam Technology and Material Modification, Institute of Low Energy Nuclear Physics, Beijing Normal University, Beijing* 100875, *China*

[b)] *Department of Materials Science and Engineering, Beijing University of Aeronautics and Astronautics*

(Received 29 June 2001; revised manuscript received 17 October 2001)

Molybdenum ions are implanted into aluminium with high ion flux and high dose at elevated temperatures of 200°C, 400°C and 500°C. Due to the high temperature and high flux of vacancies and interstitial atoms, the atom diffusion and chemical effects are enhanced during the ion implantation. The effects increase with increasing ion flux and dose, so that new phase formation and phase transition emerge noticeably. X-ray diffraction analysis shows that when the aluminium is implanted with Mo ions at a low ion flux ($25\mu A/cm^2$), the Al_5Mo alloy is formed. The atomic ratio of Mo/Al of the Al_5Mo phase is close to 20%. When the aluminium is implanted with Mo ions at a high ion flux ($50\mu A/cm^2$), the phase transition from Al_5Mo to $Al_{12}Mo$ appears, and the latter is dominant, which is determined to be the final phase. The ratio of Mo/Al in $Al_{12}Mo$ is 7.7%. Rutherford backscattering spectroscopy indicates also that the Mo/Al atom ratio is ~7% to ~8% in Mo-implanted aluminium. The atomic ratios of the constituents in Al_5Mo and $Al_{12}Mo$ are of stoichiometric composition for these alloys. The thicknesses of the $Al_{12}Mo$ alloy layers for Mo-implanted Al with ion doses of $3\times10^{17}/cm^2$ and $1\times10^{18}/cm^2$ are 550nm and 2000nm, respectively. The pitting corrosion potential V_p increases obviously. It is clear that due to the formation of $Al_{12}Mo$ alloy layer, the pitting corrosion resistance is enhanced.

Keywords: Mo-implanted Al, MoAl alloy, phase transition, pitting corrosion resistance
PACC: 6170T, 6170W, 6630J

1. Introduction

The research and application of ion implantation have been widely developed in China.[1−4] Aluminium alloys have attracted much attention due to their importance for industrial applications. These alloys enjoy good corrosion and wear resistance. Among the existing preparation techniques, ion implantation is especially well suited to preparing surface alloys on the aluminium matrix with special properties. Surface synthesis of Cr–Al, Ti–Al, Mn–Al and Mo–Al alloys by implantation has been reported.[5,6] Ion implantation has been used as an important tool for surface modification.[3] However, the projected range of the metal ions introduced by the conventional ion implantation can reach only one or two hundred nanometres. New processing techniques are always desired to achieve a much thicker modified layer, and this purpose can be reached by implantation with high ion flux and high dose.[7,8]

The metal vapour vacuum arc (MEVVA) ion implanter can produce various metal and compound ions with large ion flux and high charge state. It has been used in the modification of aluminium and steel,[9−11] and improvements of their mechanical and chemical properties have been observed. In this paper, we study the phase transition of Mo-implanted aluminium with high ion dose and ion flux. A thicker Mo–Al alloy layer is obtained by Mo ion implantation into aluminium without annealing using the MEVVA implanter. The pitting corrosion behaviour is studied for the first time, as far as we know. The mechanism of the phase transition and pitting corrosion improvement in Mo-implanted aluminium is discussed.

2. Experiment and methods

The samples used are 0.2mm Al plates with a pu-

*Project supported by the National Natural Science Foundation of China (Grant Nos 59671051 and 59871003), and by the National High Technology Development Programme of China (Grant No 863-715-023-02-01).

†Corresponding author: FAX 086-10-62231765; Tel. 086-10-62209578(H), 086-10-62207077(O).
E-mail: brc@bnu.edu.cn; zhangth@bnu.edu.cn

rity of 99.99%. Molybdenum ions are implanted using a MEVVA implanter at an average energy of 112keV in the dose range from 1×10^{17} to 1×10^{18}/cm^2. The ion fluxes are 25, 50, 67 and 125μA/cm^2. Temperature rises of the samples are 200, 400, 510 and 585°C during Mo implantation, respectively. The phase analysis was carried out by x-ray diffraction (XRD). Rutherford backscattering spectroscopy (RBS) was used to determine the Mo atom distribution in the aluminium. The implanted conditions are listed in Table 1.

3. Results and discussion

3.1. The relation between the target temperature rise and ion flux

The relation between the target temperature rise and ion flux for Mo implantation into aluminium is shown in Fig.1. It is shown that the target temperature rise increases with increasing implantation time; when it reaches 800s, the target temperature rise increases to the saturation temperature. The saturation target temperature rise increases with increasing ion flux; when the ion fluxes are 25, 50 and 67μA/cm^2, the saturation target temperature rises are 200, 400 and 510°C, respectively.

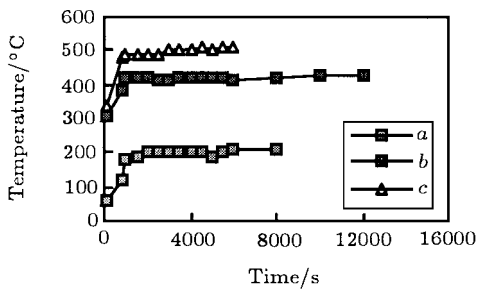


Fig.1. The relations among target temperature, implantation time and ion flux for Mo-implanted aluminium: *a*, 3×10^{17}/cm^2, 25μA/cm^2 (3mA); *b*, 6×10^{17}/cm^2, 50μA/cm^2 (6mA); *c*, 3×10^{17}/cm^2, 60μA/cm^2 (7mA).

Table 1. Relations among implantation conditions, experimental results (dose D_T, ion flux Φ, target temperature T_i), retained dose D_R, and the peak concentration N_p of Mo atoms.

No	D_T /(10^{17}/cm^2)	D_R /(10^{17}/cm^2)	T_i /°C	N_p /%	Φ /(10^{14}cm^{-2}s^{-1}/(μAcm^{-2})	D /10^{-13}cm^{2}s^{-1}
AM41	1	0.64 (64%)	400	7	2.81/(50)	0.093
AM43	3	2.0 (66%)	400	7	2.81/(50)	3.24
AM53	3	2.1 (70%)	500	7–8	4.37/(70)	7.78
AM25	5	2.0(40%)	200	19	1.56/(25)	0.27
AM46	6	4.5 (75%)	400	7	2.81/(50)	6.56
AM410	10	7.9 (79%)	400	6–7	2.81/(50)	11.50

3.2. Mo atom concentration distribution

In Mo-implanted aluminium the Mo atom profile shape is different for different ion fluxes. The Mo atom profile shape is Gaussian-like for an ion flux of 25μA/cm^2 (see curve *a* in Fig.1), and the Mo atom peak concentration is about 20%. The atomic ratio of Al to Mo is of the stoichiometric composition of the Al_5Mo alloy. It can be seen that the Mo-implanted Al probably forms the Al_5Mo alloy layer. However, if the ion flux of 50μA/cm^2 is used to implant, the Mo atom profile shape in Mo-implanted Al with a higher dose is always close to a platform over a wide region of depth distribution (see curves *b*, *c* and *d* in Fig.2). The penetration depth increases with increasing ion dose. The peak concentrations for Mo in the implanted aluminium at different ion doses with an ion flux of 50μA/cm^2 are always close to 7%–8% (see Table 1). The atomic ratio of Al/Mo is of the stoichiometric composition of $Al_{12}Mo$ alloy. This indicates that the $Al_{12}Mo$ alloy layer is formed in the implanted layer during the ion implantation. It is shown that the thickness of the MoAl alloy layer increases with increasing ion dose. The layer thicknesses for samples AMo41, AMo46 and AMo410 are 200nm, 800nm and 1100nm, respectively. The results show that a transient enhanced diffusion takes place due to the effect of the large number of point defect fluxes (vacancies, interstitials and clusters) induced during the ion implantation. These point defects facilitate the motion of Mo atoms. Therefore, the diffusion is enhanced significantly during Mo implantation into Al with high ion flux and high dose (see Table 1). The phase formation and phase structures are strongly affected by

radiation damage, radiation segregation and the enhanced diffusion of Mo ions.[7,8] The peak concentrations of Mo atoms in Mo ion implantation into Al are given in Table 2.

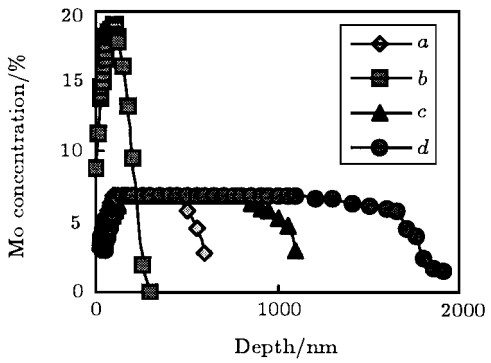


Fig.2. Concentration profiles of the Mo atoms in Mo-implanted aluminium: curve *a*, $3\times10^{17}/cm^2$, $25\mu A/cm^2$; curve *b*, $3\times10^{17}/cm^2$, $50\mu A/cm^2$; curve *c*, $6\times10^{17}/cm^2$, $50\mu A/cm^2$; curve *d*, $1\times10^{18}/cm^2$, $50\mu A/cm^2$. The energy of these samples is 112keV.

3.3. Enhanced diffusion

According to the above experimental results the enhanced diffusion coefficients can be calculated using the following equation[12]

$$N(x,t) = \frac{D_T}{(2\pi(\Delta R_p^2 + 2Dt))^{1/2}} \times \exp\left(\frac{-(x-R_p)^2}{2\Delta R_p^2 + 4Dt}\right), \quad (1)$$

where R_p and ΔR_p are the projected range and straggling, respectively. D_T is the ion dose, D is the diffusion coefficient and t is the implantation time. This equation is suitable for ion implantation with high ion flux and high dose, at elevated temperatures and post annealing. For D=0, the Mo atom distribution is as follows

$$N(x,0) = \frac{D_T}{(2\pi\Delta R_p^2)^{1/2}} \exp\left(\frac{-(x-R_p)^2}{2\Delta R_p^2}\right). \quad (2)$$

This formula is suitable for low ion flux and low dose implantation. The diffusion coefficient D can be obtained using both the above equations, and it is expressed as[13]

$$D = \frac{1}{2t}\left[\left(\frac{\Delta x}{(-2LnQ)^{1/2}} + \Delta R_p\right)^2 - \Delta R_p\right], \quad (3)$$

where $\Delta x = x_2 - x_1$. Usually, $Q = N_2\ (x_2,t)/N_{p2} = N_1(x_1,0)/N_{p1}$=0.5, N_{p1} and N_{p2} are the peak concentrations corresponding to Eqs.(1) and (2), respectively. $N_1(x_1,0)$ and $N_2(x_2,t)$ are the atom concentrations at Q=0.5, corresponding to Eqs.(1) and (2), respectively. x_2 and x_1 are the coordinates on the x-axis corresponding to Eqs.(1) and (2) at Q=0.5, respectively.

The diffusion coefficient D obtained from these values can be calculated by using Eq.(3). The results are listed in Table 1, and the relation between D and ion flux is shown in Fig.3. It is found from Table 1 and Fig.3 that the diffusion coefficient of Mo atoms in Al increases with the increasing Mo ion flux and dose. The diffusion coefficient of sample AM410 is 2.6 times higher than that of sample AM43. The maximum value of the average diffusion coefficient is $3\times10^{-12}cm^2/s$ (Am410) and the minimum is $9.3\times10^{-15}cm^2/s$ (AM41). The diffusion coefficient of AM410 is 124 times greater than that of AM41, and 42.6 times greater than that of AM25. The diffusion coefficient of AM53 is 1.4 times higher than that of AM43.

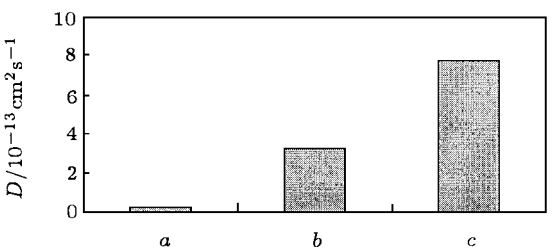


Fig.3. The relation between diffusion coefficients and ion flux for the Mo-implanted aluminium: *a*, $25\mu A/cm^2$, $5\times10^{17}/cm^2$; *b*, $45\mu A/cm^2$, $3\times10^{17}/cm^2$, $50\mu A/cm^2$; *c*, $70\mu A/cm^2$, $3\times10^{17}/cm^2$.

3.4. XRD analysis

XRD analysis can give information of the new phase formed in the Mo-implanted layer. The XRD pattern of pure aluminium shows that diffraction peaks of the crystal faces of (111), (200), (220), (311) and (331) of pure aluminium are clearly shown. After Mo implantation to a dose of $1\times10^{17}/cm^2$ with an ion flux of $50\mu A/cm^2$, some small diffraction peaks of $Al_{12}Mo$ and Al_5Mo appear in the diffraction pattern.

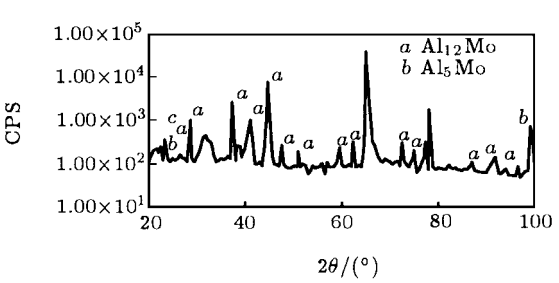


Fig.4. XRD spectrum of the Mo-implanted (AM46) aluminium.

If an ion dose of $6\times10^{17}/cm^2$ is used for the implantation with an ion flux of $50\mu A/cm^2$ (AM46), more diffraction peaks of $Al_{12}Mo$, $AlMo_3$ and Al_5Mo can appear in the diffraction pattern, as shown in Fig.4. The diffraction peak intensity of the $Al_{12}Mo$ phase increases with increasing ion dose. But the diffraction peak intensity of the Al_5Mo phase is minimal, and the diffraction peak intensity of the $AlMo_3$ phase disappears already. That is to say, the phase transition process is observed. The results are listed in Table 2. It can be seen from Fig.4 and Table 2 that $MoAl_3$ and $Al_{12}Mo$, $AlMo_3$ and Al_5Mo phases are formed during the implantation.

Table 2. The relation of diffusion coefficients D under the implanted conditions, with Q=0.5 (dose D_T, ion flux Φ, target temperature T_i), retained dose D_R, and Mo atom peak concentration N_p.

No	D_T /(10^{17}/cm^2)	D_R /(10^{17}/cm^2)	T_i /°C	N_p /%	Φ /10^{14}cm^{-2}s^{-1}/(μAcm^{-2})	Phase
AM41	1	0.64 (64%)	400	7	2.81/(50)	$Al_{12}Mo$, Al_5Mo
AM43	3	2.0 (66%)	400	7	2.81/(50)	$Al_{12}Mo$
AM53	3	2.1 (70%)	510	7–8	4.37/(70)	$Al_{12}Mo$
AM25	5	2.0(40%)	200	19	1.56/(25)	$Al_{12}Mo$,Al_5Mo, $Al8Mo_3$
AM46	6	4.5 (75%)	400	7	2.81/(50)	$Al_{12}Mo$
AM410	10	7.9 (79%)	400	6–7	2.81/(50)	$Al_{12}Mo$

The relations between the diffraction peak intensity and ion dose are given in Fig.5. Curves *a* and *b* in Fig.5 show the relations between the diffraction peak intensity and ion dose for phases $Al_{12}Mo$ (101) and Al_5Mo (112), respectively. It is shown that the diffraction peak intensity for $Al_{12}Mo$ increases noticeably with increasing ion dose (curve *a* in Fig.5), but the change of diffraction peak intensity for the Al_5Mo phase is minimal, as shown in curve *b* in Fig.5. These results indicate that a mixed growth of phases would occur in the case of Mo-implanted aluminium with an ion flux of $50\mu A/cm^2$. But the phase of $Al_{12}Mo$ is dominant. There are some diffraction peaks of the phases MoAl and Al_2O_3 in these samples. The XRD analysis for Mo-implanted aluminium at an ion flux of $25\mu A/cm^2$ shows that the mixed growth of the above stated phases would also occur, but the phase Al_5Mo is dominant (see Table 2). These results agree with the above-mentioned RBS analysis.

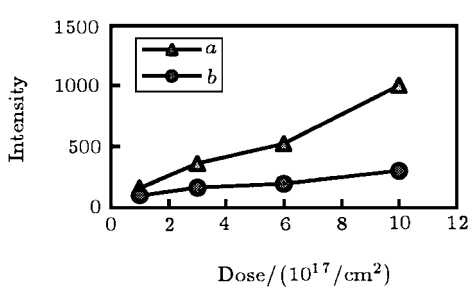


Fig.5. The relations between diffraction peak intensity and ion dose for Mo-implanted samples: *a*, $Al_{12}Mo$ (311); *b*, Al_5Mo (111).

3.5. Pitting corrosion behaviour

The pitting corrosion resistance of aluminium is improved obviously by Mo implantation into aluminium. Relations of pitting corrosion potential and corrosion current density for aluminium, AM41, AM46 and AM410 are measured in a solution of 0.1N NaCl. The results are shown in Fig.6. For aluminium, AM41, AM46 and AM410 their pitting corrosion potentials are −585mV, −560mV, −450mV and −360mV respectively. The pitting corrosion potentials of AM41, AM46 and AM410 are 25, 135 and 225mV higher than that of aluminium respectively. The increase of pitting potential will enhance the corrosion resistance noticeably. This means that a very good passivation layer against pitting corrosion has been formed by the Mo implantation. The passivation layer consists of Mo alloys and metallic oxides.

It is well known that the subjects for enhanced diffusion are vacancies, interstitial atoms and defects in solids. A high-density flux of vacancies and interstitial atoms are formed during Mo implantation. When molybdenum is implanted into aluminium at an average energy of 112keV, the vacancy density induced by one ion can be calculated by the TRIM95 program, and is 814 vacancies/ion. The amount of interstitial atoms is also 814 vacancies/ion. If the ion flux is $50\mu A/cm^2$ ($2.81\times10^{14}cm^{-2}s^{-1}$) (see Table 1), the vacancy flux J_v=$2.6\times10^{17}cm^{-2}s^{-1}$. It can be seen from Table 1 that the vacancy flux and interstitial atom flux increase with increasing ion flux. Owing to the intense atom collision cascades, a powerful flux

of vacancies and interstitial atoms, dislocations and a local temperature rise are produced. Therefore, the diffusion coefficient increases greatly due to the reaction between these defects and the Mo atoms, and then the motion of Mo atoms and the formation of alloy phases are also enhanced. So the Mo atom diffusion coefficient increases with increasing ion flux and ion dose. A deeper implantation layer of 2000nm is thus obtained during implantation with an ion dose of $1\times10^{18}/\mathrm{cm}^2$. It can be seen that the radiation-enhanced diffusion of Mo atoms in aluminium causes a "long-range diffusion effect". Therefore, the Mo retained dose in aluminium increases noticeably with the increase of the ion flux, obtained during implantation with an ion dose of $1\times10^{18}/\mathrm{cm}^2$. It can be seen that the radiation-enhanced diffusion of Mo atoms in aluminium causes a "long-range diffusion effect".

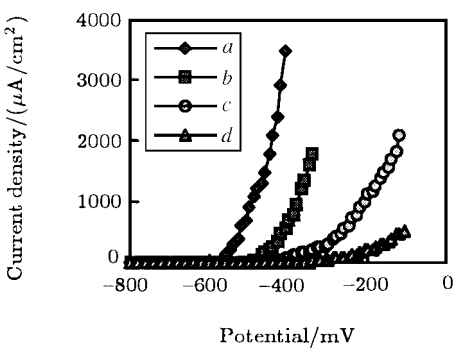


Fig.6. The relations between current density and pitting potential for aluminium and Mo-implanted aluminium: *a*, aluminium; *b*, $1\times10^{17}/\mathrm{cm}^2$, $50\mu\mathrm{A}/\mathrm{cm}^2$; *c*, $6\times10^{17}/\mathrm{cm}^2$, $50\mu\mathrm{A}/\mathrm{cm}^2$; *d*, Mo $1\times10^{18}/\mathrm{cm}^2$, $50\mu\mathrm{A}/\mathrm{cm}^2$.

4. Conclusions

The phase transition, deep alloy layer formation and pitting corrosion behaviour have been studied. The main results are summarized as follows.

The Mo atom profile shape is Gaussian for the Mo-implanted aluminium with an ion flux of $25\mu\mathrm{A}/\mathrm{cm}^2$ and a dose of $3\times10^{17}/\mathrm{cm}^2$. If an ion flux of $50\mu\mathrm{A}/\mathrm{cm}^2$ is used to implant, the Mo atom profile shape is close to a platform over a wide depth distribution region.

The Mo atom peak concentration is high for Mo-implanted aluminium with an ion flux of $25\mu\mathrm{A}/\mathrm{cm}^2$. When an ion flux of $50\mu\mathrm{A}/\mathrm{cm}^2$ is used, the peak concentrations for the Mo-implanted aluminium at different ion doses are always close to 7%–8%. The atomic ratios Mo/Al of 20% and 7%–8% are the stoichiometric compositions of Al_5Mo and $Al_{12}Mo$ alloys, respectively.

The result of XRD analysis agrees with that of RBS for the phase formation. The phase transition process from Al_5Mo to $Al_{12}Mo$ has been formed.

The penetration depth increases with increasing ion flux and dose. The $Al_{12}Mo$ alloy layer is formed in the implanted layer during ion implantation, and the layer thicknesses for samples AMo41, AMo64 and AMo410 are 200nm, 800nm and 2000nm, respectively.

The diffusion coefficient of Mo atoms in Al increases with increasing Mo ion flux and dose. The maximum value of the average diffusion coefficient is $3\times10^{-12}\mathrm{cm}^2/\mathrm{s}$(Am410), and the minimum value is $9.3\times10^{-15}\mathrm{cm}^2/\mathrm{s}$ (AM41).

After Mo implantation, the pitting corrosion resistance has been improved. The pitting corrosion potentials of AM41, AM46 and AM410 are respectively 25, 135 and 225mV higher than that of aluminium.

References

[1] Zhang T, Kwok T K, Chu P K and Brown I G 2001 *Chin. Phys.* **10** 320

[2] Zhang T H, Wu Y G, Sang H B, Li Y L and Zhou G 2001 *Chin. Phys.* **10** 295

[3] Lu T 2001 *Chin. Phys.* **10** 145

[4] Wang Y G 1997 *Chin. Phys.* **6** 746

[5] Sanchez F H, Namavar Ff, Budnick J I, Fasihuddin A, Koch C H and Hayden H C 1987 *Mater. Sci. Eng.* **90** 149

[6] Da Sila R C, Sousa R C, Conde O, de Sila M F and Soarres J C 1996 *Surf. Coat. Technol.* **83** 60

[7] Yang J H and Zhang T H 1997 *Chin. Phys. Lett.* **14** 865

[8] Friedland E, ven der Berg N G, Hanβmann J and Mayer O 1996 *Surf. Coat. Technol.* **83** 10

[9] Zhang T H, Ji C Z, Shen J H, Yang J H and Chen J 1991 *Nucl. Instrum. Methods* B **59/60** 828

[10] Zhang T H, Wu Y G, Zhao Z Y and Deng Z W 1999 *Chin. Phys. Lett.* **16** 196

[11] Qian W D and Zhang T H 1996 *Function Materials Proc. C-MRS'96'* I-3 (Beijing) p 443

[12] Seidel T 1969 *Trans. Metall. Soc. AIME* **245** 491

[13] Zhang T H and Wu Y G 1999 *Science and Application of Ion Beam Modification of Materials* (Beijing: Science Press) pp 44-45 (in Chinese)